ACS APPLIED MATERIALS & INTERFACES

Functional Nanostructured Materials (including low-D carbon)

Nanoscale Homogeneous Energetic Copper Azides@Porous Carbon Hybrid with Reduced Sensitivity and High Ignition Ability

Rui Xu, Zhenzhan Yan, Li Yang, Qianyou Wang, Wenchao Tong, Naimeng Song, Jimin Han, and Yang Zhao

ACS Appl. Mater. Interfaces, **Just Accepted Manuscript** • DOI: 10.1021/acsami.8b04317 • Publication Date (Web): 08 Jun 2018

Just Accepted

ACS Publications

is published by the American Chemical Society. 1155 Sixteenth Street N.W., Washington, DC 20036

Nanoscale Homogeneous Energetic Copper Azides@Porous Carbon Hybrid with Reduced Sensitivity and High Ignition Ability

Rui Xu ,[†1] Zhenzhan Yan[†1], Li Yang[†], Qianyou Wang[†], Wenchao Tong[†], Naimeng Song[†], Ji-Min Han[†] and Yang Zhao[‡]*

[†]State Key Laboratory of Explosion Science and Technology, Beijing Institute of Technology, Beijing, 100081, P.R. China

[‡]School of Chemistry and Chemical Engineering, Beijing Institute of Technology, Beijing, 100081, P.R. China

KEYWORDS: Faraday cage, porous carbon, energetic material, electrostatic sensitivity, ignition ability

ABSTRACT

Researching on green primary explosives with lead-free and excellent ignition performance is of significance for practical applications. In this work, we have developed a novel, green and facile strategy to synthesize copper azide@porous carbon hybrids (CA@PC) based on ionic crosslinked hydrogel with the low-cost cellulose derivatives as starting material, in which the CA nanoparticles are uniformly distributed in the porous carbon skeletons. The detailed

characterizations and control experiments demonstrated that such outstanding performance origins from the excellent electric conductivity of nano-scale carbon cages. With the favorable unique structures, the as-prepared hybrids can greatly benefit the new type of energetic materials, which exhibit much low electrostatic sensitivity of 1.06 mJ. Interestingly, it possesses the high ignition ability and the flame sensitivity can even achieve 47 cm, superior to those well-developed CA based materials reported previously. This work paves the way toward the designing and developing next generation highly efficient energetic materials.

1. Introduction

The solid energetic materials, especially nitrogen-rich salts and compounds, are sensitive and powerful primary explosives. Among them, the energetic materials containing lead, such as lead azide (LA) and lead styphnate (LS), are the most-used effective and reliable primary explosives at present, which have been utilized in almost all chemical detonators.[1] However, due to the high toxicity[2] and weak power for Micro-Electro-Mechanical System (MEMs),[3,4] a large numbers of researches are inspired by utilization of novel complex based on typical nitrogen-rich heterocycle ligands, including 1,1-di(nitramino)tetrazole and 4,5-bis(dinitromethyl)furoxanate derivatives.[5-8] Nevertheless, owing to the complex synthesis paths and conditions, high cost and environment factors, these energetic materials are still restricted in practical application. Therefore, it's urgent to develop environmental-friendly, easily-prepared and high-level powerful energetic materials as primary explosive to balance the sensitivities and explosive performances.

As an environment-friendly and brisance energetic material, CA has attracted much attentions recently.[9-12] However, the inherent high mechanical and electrostatic sensitivity hinder its further practical applications.[12] Although many efforts have been devoted to constructing various CA

based materials to reduce the mechanical and electrostatic sensitivity,[13-15] including the synthesis of CA based composites by mixing with carbon materials (graphene, graphite or activated carbons), and the CAs confined into the inside of carbon nanotubes,[16-18] it is still difficult to realize highly dispersion of CA in the composite systems to achieve high efficient and security primary explosive.

Porous carbon with high specific surface, excellent mechanical and thermal properties is regarded as promising candidate support materials, which provides amounts attachment sites for CAs loading on carbon skeletons and can be prepared easily from some cheap raw materials, such as sodium alginate (SA),[19] cellulose[20] and cellose-derived materials, by a template-free chemical carbonization process. [21,22] Besides, the honeycomb structural units of porous carbon act as conductive explosion-proof cages (like Faraday cages: an enclosure used to block electromagnetic fields) for the sensitive energetic materials because that an external electrical field would cause the uniform distribution of electric charges within the cage's conducting material (such as carbon frameworks) leading to eliminating the field's effect of the internal cages. When the electrostatic charges are transferred onto the surface of the sample, it would be conducted along with the carbon framework as an electrostatic shield. Therefore, introducing CAs into these nano-scale Faraday cages will largely decrease the electrical sensitivity of the whole system. In this regard, we have developed an efficient strategy to create the uniform dispersion of CA on carbons with the enhanced efficiency of azidation and reduced electrical sensitivity, which is of significance for the future practical applications.[18] Therefore, to satisfy the increasing demands for green and safe primary explosives, the effort on exploring and researching new fabrication routes for high efficient and secure CA based explosives is urgent, which is still challenging.

Herein, we reported a novel three-step synthetic pathway to facilely fabricate copper azide-porous carbon (CA@PC) hybrids based on ionic crosslinked hydrogel using low-cost cellulose derivatives as starting material, in which CAs are uniformly distributed on porous carbon skeletons. By means of this strategy, the CA@PC material is formed with much low electrostatic sensitivity of 1.06 mJ. Moreover, its flame sensitivity can achieve 47 cm, showing a higher ignition ability than those previous reported CA based composite materials. This work provides the opportunity for the facile construction of next generation energetic materials with high performance and security in various functional energy-related fields.

2. Result and Discussion

The schematic synthesis process of CA@PC is illustrated in Figure 1. For preparation of CA@PC, the cupric carboxymethyl celluloses (CMC-Cu) hydrogel is first prepared with cupric acetate as ionic crosslinker without any organic solution (Figure 1a, b), [23-34] in which the metal ions can be well dispersed in the organic molecular chains, similar to the metal organic frames (MOFs).[35-40] The detailed process and characterization are shown in supporting information (Figure S1–S4).[20-31,41-43] Considering the slightly ionic-linked hydrogel swelling would lead to the continued increasing of water content in the whole system until achieving the equilibrium between H_3O^+ (including H^+ ionized from water) and the metal ionics (Al^{3+}, Ca^{2+} or Fe^{3+}) binding on hydrophilic groups like –COOH on polymer chains which results in the mechanical instability and the considerable loss of Cu^{2+} of hydrogel, the CMC-Cu hydrogel is cross-linked by adding excess Cu^{2+} which acts as coordination sites with carboxyl of CMC chains, leading to a well-dispersion of Cu^{2+} in hydrogel networks (Figure S2). Interestingly, the as-formed CMC-Cu hydrogel exhibits high swelling resistance as a result of excessive ionic-linking also shows self-healable action to a certain extent during the purifying process (Figure S1).[23-25] Moreover,

the residual Na^{+}, CH_3COO^{-} and Cu^{2+} of the obtained CMC-Cu hydrogel can be directly removed by simple rinse-standing treatment, which is totally different with the conventional post process. After lyophilization, the obtained CMC-Cu hydrogel is then carbonized at 400 ^{o}C for 2 h under nitrogen flow.[44,45] During this process, the copper nanoparticles are gradually doped into carbon frameworks to form the Cu-porous carbon (Cu@PC) composite (Figure 1c). Detail characterization and morphology of Cu@PC are shown in support information (Figure S5–8 and Table S1). Finally, the CA@PC product with CAs highly distributed on the porous carbon frameworks (Figure 1d) is successfully obtained without any by-products through azidation reaction process (Figure S10-12).[46-49]

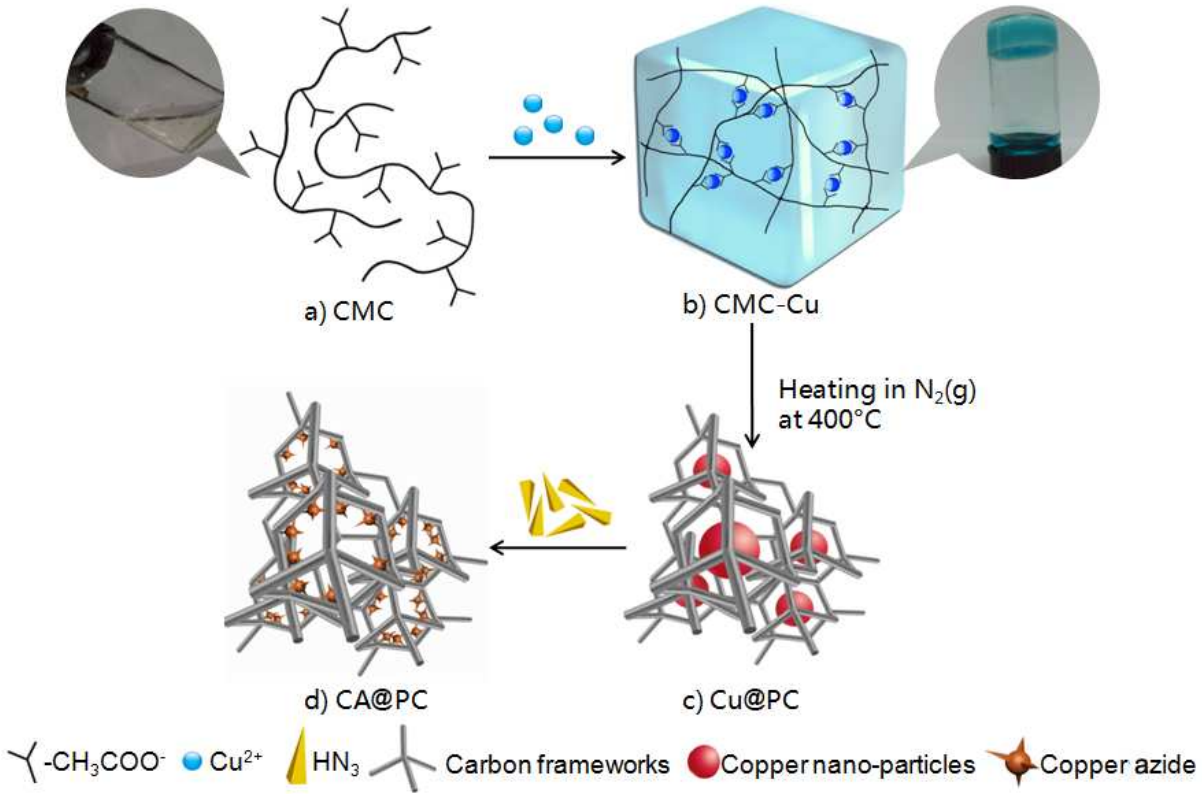

Figure 1. a) The molecular structure of commercial carboxymethyl cellulose (CMC), inset is the digital of CMC solution; b) ionic-linked hydrogel prepared from CMC and Cu^{2+} (CMC-Cu), inset is the digital of the formed hydrogel; c) Cu nano-particles well-distributed in carbon

frameworks (Cu@PC); d) CA nano-crystals adhering to the carbon frameworks (named as CA@PC).

The transmission electron microscope (TEM) images in Figure 2a–d show the porous nanojunction structures of CA@PC with nanosheets cross-linking together. The typical scanning transmission electron microscopy (STEM) images (Figure 2e and S13) reveal that the C, O, N and Cu elements are uniformly distributed all over the as-prepared CA@PCs basal plane, consistent with the TEM images (Figure 2d). Besides, the content of $Cu(N_3)_2$ obtained from coupled plasma atomic emission spectrometry (ICP) data is about 56.40%, in which the N content is 32.11%, much higher than LA (28.86%). The X-ray diffraction (XRD) spectra of CA@PCs exhibit the typical $Cu(N_3)_2$ patterns (Figure 2f), suggesting the successful azidation reaction process for Cu@PCs. In contrast, the peaks related to copper disappeared, indicating the copper are completely transformed into CAs without any by-products (such as cuprous azide). From the XPS data of the final product, it can be seen that the sample only contains CA/C without other impurities (Figure S12). The differential scanning calorimeter (DSC) curve in Figure 2g exhibits a sharp peak at 210 ^{o}C according to thermal decomposition of CA, also confirming the successful transformation of copper into CA. In addition, thermal properties of $Cu(N_3)_2$ in CA@PC composite are also investigated, which still keeps its ignitability. The peak at 342 °C is related to decarboxylation and oxygen reduction of detonation product, which could also be found on the DSC curve of CA@PC (Figure 2g) and the DSC curve of Cu@PC (Figure S9). It means that during ignition process, there will be extra energy released besides the explosion of CA. The CA@PC exhibits relative high density of 1.85 g cm^{-3} measured by helium displacement methods, and the heats of formation process of CA@PC is calculated to be

*ca.*1392.88 kJ mol^{-1} (or 2.68 MJ kg^{-1}). Detail method and data on the calculations are given in the Supporting Information (Section 1).

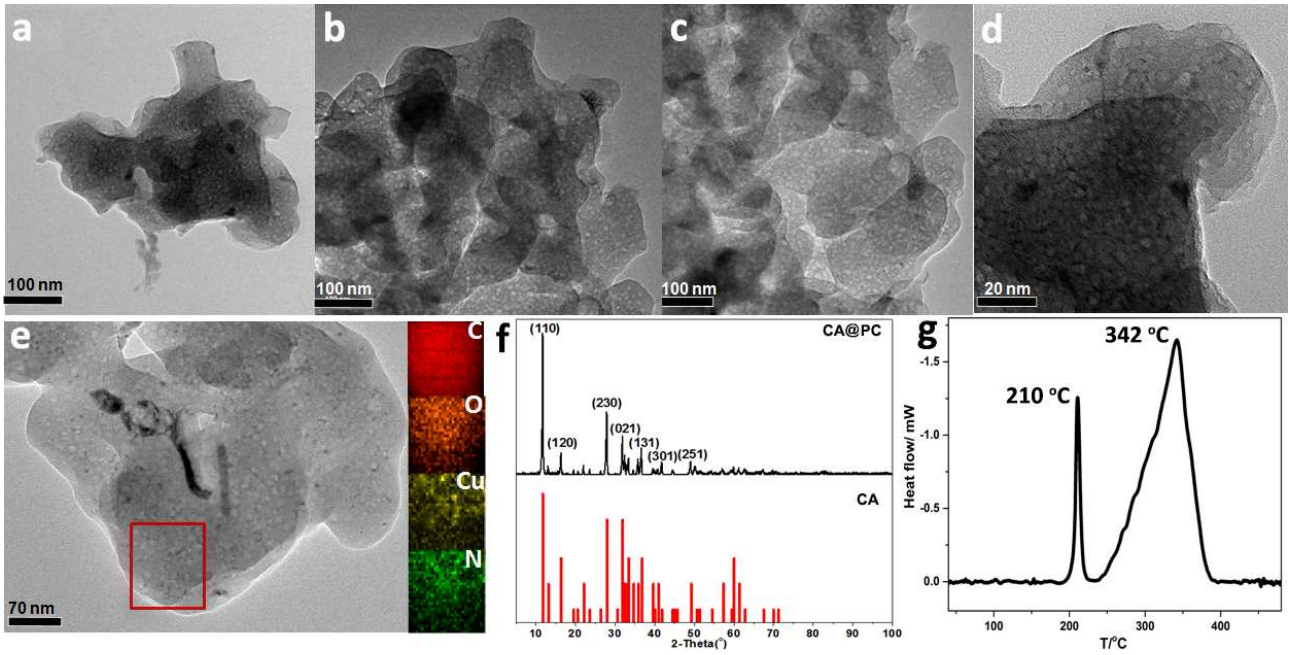

Figure 2. a–d) TEM images; e) energy dispersive X-ray spectroscopy (EDS) mapping; f) P-XRD pattern (JCPDS card No. 21-0281) and g) DSC curve of CA@PC.

In order to evaluate the stability and ignition performance, the electrostatic and flame sensitivity of CA@PC are investigated (Figure 3). For comparison, the mixtures of LA/LS and the CA/carbon (CA/C) composites are also prepared under the similar conditions (Figure 3). Sensitivity test and explosive test are carried out by the same methods and equipments reported in our recent work.[13,18] The electrostatic sensitivity of CA@PC is tested by observing its safety under a certain amount of electrostatic stimulus, shown as E_{50} (the energy for 50% probability of ignition, mJ). Interestingly, electrostatic sensitivity of CA@PC in Figure 3b is about 1.06 mJ, much lower than those mixtures containing lead, which are 0.23 (LA/LS=1:2), 0.61 (LA/LS=1:3) and 0.1 mJ (LS), respectively, and far lower than the electrostatic sensitivity of CA (0.05 mJ) (Figure 3d). In comparison with those of physically mixed CA/C composites, including wet-

impregnated and vacuum-impregnated products (CA content is 45%), CA@PC can keep low electrostatic sensitivity with higher content of CA (Figure 3d and S14). The flame sensitivity, related with ignition ability, is shown as H_{50} (the height from standard black powder pellets to sample for 50% probability of ignition, cm). Interestingly, flame sensitivities of all the three well-dispersed CA/C composites, including CA@PC, MOF-CA (Copper azide and carbon composite prepared by MOF template method) and VC/CA (Copper Azide Mixed with Activated Carbon by Vacuum Impregnation), are higher than those of physically-mixed CA/C composites and LA/LS (Figure 3c and e), indicating that carbon frameworks could improve thermal conductivity rate[50] of the whole system, leading to the easy ignition. Different with the negative impact on ignition performance caused by doping carbon (only pure carbon), CA@PC exhibits the outstanding ignition ability, in which its H_{50} can reach 47 cm, even higher than CA (45 cm) and MOF-CA (42 cm). In fact, when the height is changed into 52 cm (H_{50} of LS, which is usually used as ignition composition), the ignition probability of CA@PC still reaches as high as 38%, indicating the excellent ignition ability. Considering both electrostatic sensitivity and flame sensitivity, CA@PC has a good performance on safety and ignition ability compared with common primary explosive (Figure 3f).

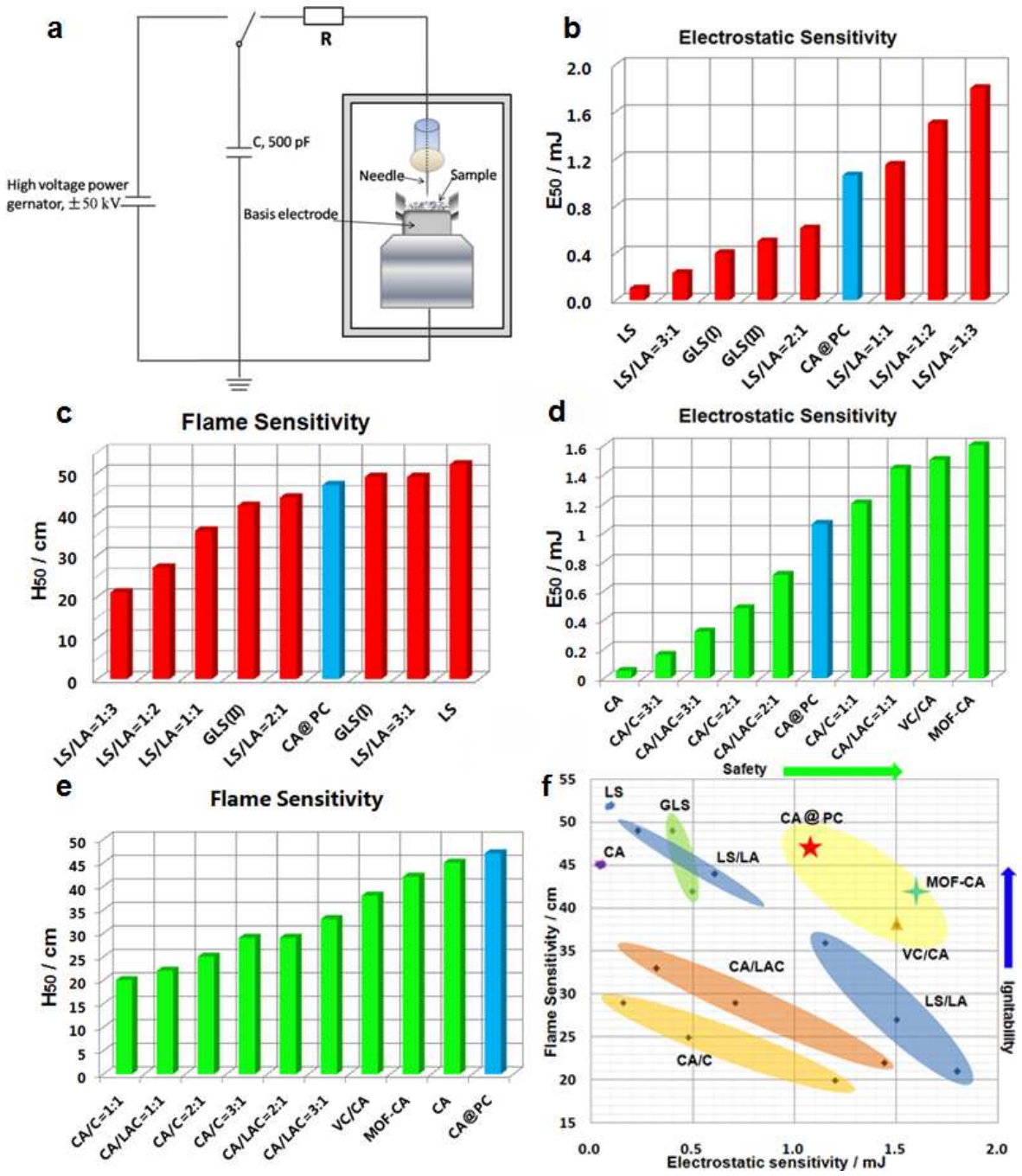

Figure 3. (a) Schematic of the electrostatic sensitivity tester; b) electrostatics sensitivities and c) flame sensitivities of CA@PC and mixtures of LA and LS, respectively; d) electrostatics sensitivities and e) flame sensitivities of CA@PC, CA, MOF-CA, CA/C, and VC/CA; f) The whole sensitivities comparison of CA@PC, mixtures of LA/LS and CA/C.

As shown in Figure 4, the mechanism of reduction of electrostatic sensitivities in CA@PC and other CA/C composites are proposed. It is believed that the electrostatic sensitivity of CA based primary explosive increases with the increase aggregation percentage of CA. Therefore, electrostatic charges built by simply mix up the CA and carbon materials couldn't conduct timely, especially on the part of CA separated with carbon, probably due to the uneven distribution of CA in carbon skeleton. In contrast, as nano-scale Faraday cages, the unique porous carbon frameworks decorated with well-dispersed CA nanoparticles can effective control the sensitivity and preserve its power, as well as reduce its liability to ignition caused by small amount of electrostatic charges, thus leading to the high safety of whole system. Besides direct physical mixing and impregnation, the enhanced physical-mixed CA/C composite is also prepared to validate this idea based on vacuum-impregnated precursor (VC/CA). The corresponding TEM images and EDS mapping of VC/CA are shown in Figure S15. Evidently, most CA and C are distributed separately with only little amount of CA overlapped in the carbon frameworks. Therefore, combined with electrostatic sensitivity data and CA content, it indicates that the dispersion degree of CA among carbon frameworks is the key to reduction of electrostatic sensitivities.

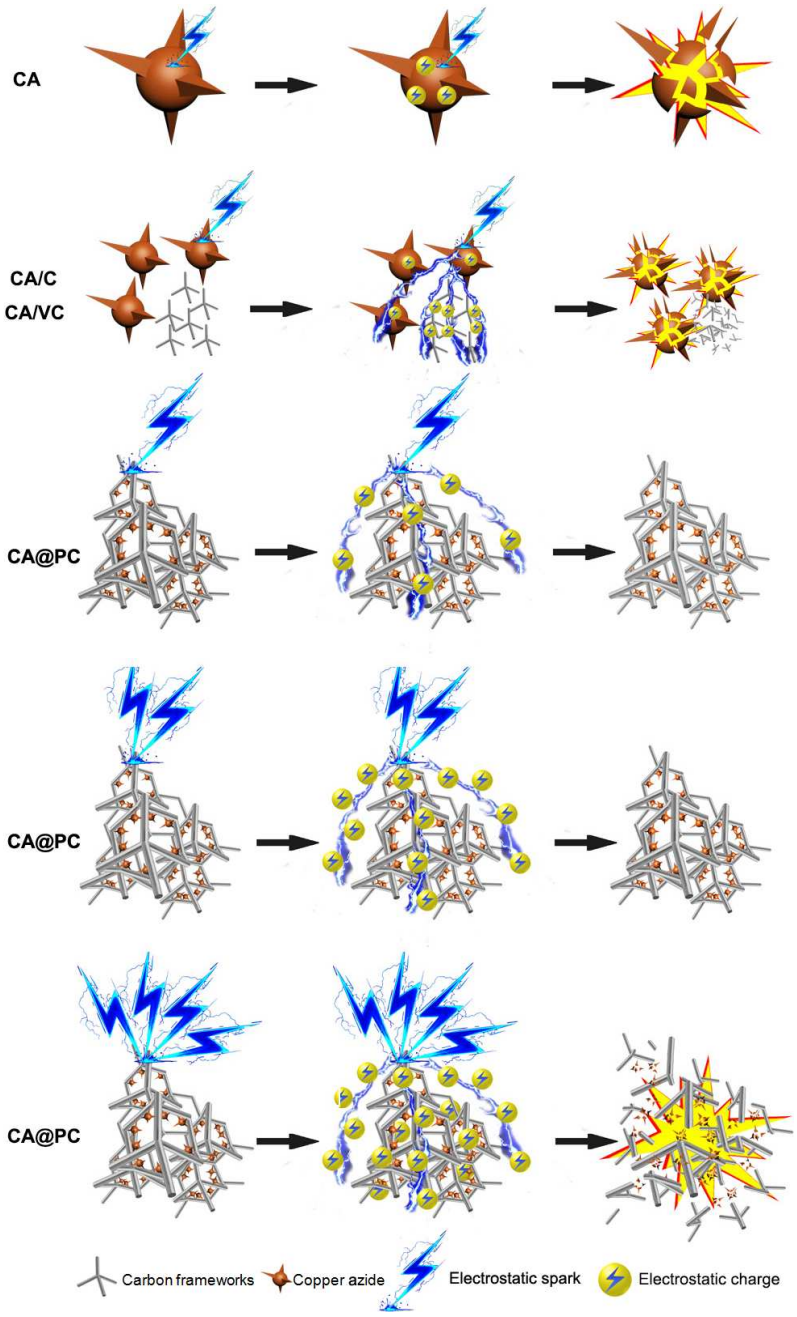

Figure 4. Schematics illustration of the mechanism of electrostastic sensitivity for CA, CA/C and CA@PC.

The ignition process of CA@PC is recorded by high-speed photography at a ratio of 2000 fps (Figure 5 and Movie S1). It can be seen that the time between the spark contacting sample and explosion is less than 10 ms, which also proves to some extent that it has good ignition capability.

Specifically impact sensitivity and friction sensitivity are both determined using the BAM drop hammer method and friction tester, respectively. The impact sensitivity of CA@PC is 1 J, and the friction sensitivity of CA@PC is 5 N. These values are comparable to those of LA and high performance primary explosives reported.[5-8,51-53] Therefore, the unique porous carbon framework makes the CA nanoparticles more accessible and much safer during preparation and transportation.

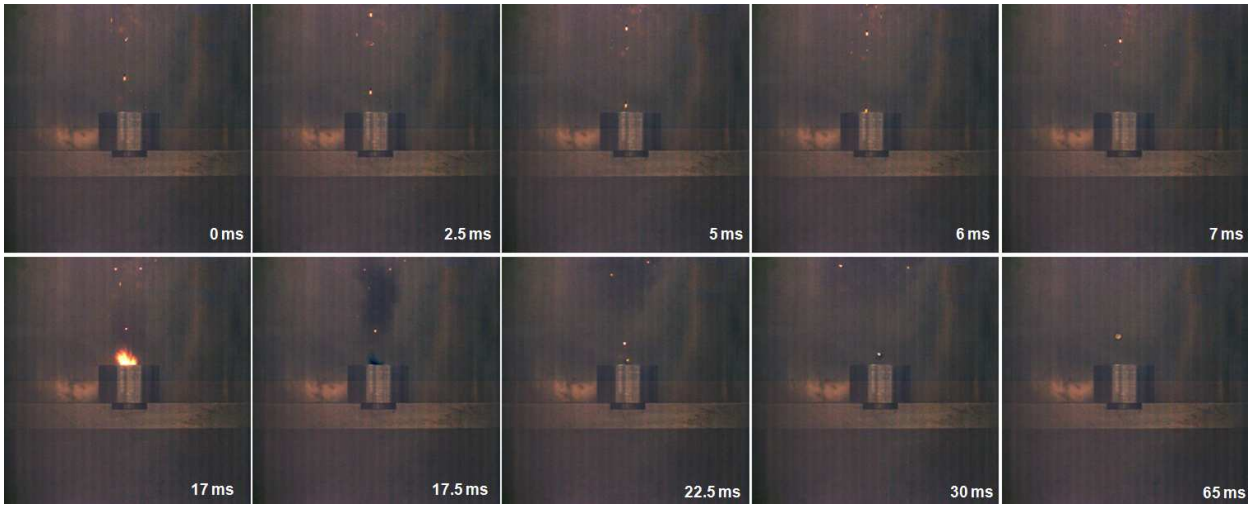

Figure 5. The ignition process of CA@PC during flame sensitivity test. The spark droped into the copper cap carring 10 mg CA@PC in the initial 7 ms. After 10 ms, the sample was ignited successfully and pushed the copper cap away.

3. Conclusion

In summary, we have demonstrated a novel three-step synthetic pathway to facilely fabricate the CA@PC hybrids, in which CAs are uniformly distributed on oxygen-rich porous carbon skeletons. The as-prepared CA@PC material exhibits much low electrostatic sensitivity and high ignition ability with the flame sensitivity of 47 cm, superior to most of reported CA based composites. This work provides new opportunities for the construction of energetic materials as well as other composite involving carbon and metal (in metal oxide) in various functional energy-related fields.

4. Experimental Section

Materials: Sodium carboxymethyl cellulose (CMC, MW=90000, DS=0.7, 50-100mpa s) is purchased from Aladdin. Copper acetate monohydrate ($Cu(OOCCH_3)_2 \cdot H_2O$, $Cu(OAc)_2$), acetic acid and Stearic acid were of analytical grade and purchased from Beijing Chemical Works. Sodium azide was analytical grade and purchased from Xiya Reagent. Other chemicals were of analytical grade and used without further purification. All solutions were prepared with distilled water.

Synthesis of CMC-Cu hydrogel: 3 g CMC was dissolved in 50 ml distilled water under stirring to make sure CMC is totally dissolved. Then 0.5 ml acetic acid was added under stirring to keep the system slightly acidic. 4 g Copper acetate was dissolved in 60 ml distilled water, and the solution was added into the CMC system drop by drop to achieve the gelation. After treated by ball mill, the homogenate of CMC-Cu hydrogel particles was allowed to stand overnight for self-healing and collected. The hydrogel was rinsed in distilled water under ultrasonic or ball-milling at room temperature to make sure it became homogenate again. Then the homogenate was

allowed to stand for at least 10h or be centrifuged in low speed. Then supernatant was taken away. The hydrogel left was used to repeat this step several times in order to wash away impurity ions, like Cu^{2+}, Na^{+} and CH_3COO^{-}. The spearmint powder was collected after lyophilization and gringing.(Figure S16a,b) T_{dec} (5 °C min^{-1}): 250.6 °C, 313.1 °C; IR (KBr): 3383 (m; ν(H–O)), 2891 (w; $\nu(CH_2)$), 1594(s; ν_{as}(C=O)), 1415 (m; ν_s(C=O)), 1335(m; ν_s(C=O)), 1056(vs; ν(1,4-glycosidic)). Anal. calcd for $(C_{148}H_{208}O_{122}Cu_7)_n$: C 40.55, H 4.78; found: C 40.37, H 4.27.

Preparation of in-situ Cu nanoparticles doping in porous carbon frameworks (Cu@PC): The freeze-dried CMC-Cu gel powder was carbonized with a nitrogen flow at 400 °C for 2h. The Heating rate was 10 °C min^{-1}. The produce was cooled down naturally to room temperature. The resulting loose powder in dark brown was needed to keep dried for azidation. (Figure S16c, d) Pore size distribution was measured by nitrogen adsorption–desorption tests carrying out at 77 K using a ASAP 2020 V4.02 (Micromeritics, USA). T_{dec} (5 °C min^{-1}): 339.1 °C; IR (KBr): 2923 (w; ν(C–H)), 1704 (s; ν_{as}(C=O)), 1602 (m; ν_{as}(C=O)).

Preparation of in-situ copper azides@porous carbon hybrid (CA@PC): The gaseous hydrazoic acid was generated by heating a mixture of sodium azide with excess stearic acid at more than 120 °C. The mixture was set in a round-bottom three-neck flask on the side neck equipped with an argon gas inlet valve and a stopper. The middle neck was equipped with an adaptor containing about a drying top-opened reagent tube. The powder was randomly deposited in the reagent tube held by a group of cotton wool for more surface area exposure to HN_3 gas. The adaptor was connected to a KOH solution as a scrubber for the unreacted HN_3 gas. After the reaction was over, the KOH scrubber solution was connected with ceric ammonium nitrate solution to neutralize the azide discharged with an argon flow. ***Caution***! Hydrazoic acid is highly ***toxic*** and metal azides are always ***energetic*** and especially ***sensitive***. The entire system must be

set up behind an explosion proof shield in a well-ventilated hood.[17,18,47] The obtained black fluffy powder should be taken lightly.(Figure S16e,f). T_{dec} (5 °C min^{-1}): 210.8, 342.0 °C.

Preparation of physically mixed VC/CA composite based on vacuum-impregnated precursor: 100mg Carbon were added into 10ml saturated copper acete solution (containing 0.72g copper acete) and string under vacuum. After washed with ethanol and dried overnight, this sample was also treated in a tube furnace at 400 °C for 2h in order to obtain physically mixed C-Cu composite.[44,45] After azidation, VC/CA(Copper Azide Mixed with Activated Carbon by Vacuum Impregnation) composite was finally prepared.

Electrostatic sensitivity test: The test parameters: the charge capacitance is 500 pF, the electrode gap length is 0.12 mm. The test energy was given by the formula:

$$E=\frac{1}{2}CV^2 \quad (1)$$

where C is the capacitance of the capacitor (Farads, F); V is charge voltage(volt, V). Samples were tested using the up and down method for each condition, and the electrostatic sensitivity (E_{50}) for 50% probability of ignition was calculated. A schematic of the apparatus used is shown in Figure 3a.

Flame sensitivity test: 20 mg of the complex was compacted to a copper cap under the press of 39.2 MPa and was ignited by black powder pellet. Samples were tested using the up and down method for each condition, and the flame sensitivity (H_{50}) for 50% probability of ignition was calculated.

Characterizations: SEM and TEM were performed using S-4800 (HITACHI, Japan) at 15kV with a point resolution of 1.0 nm and Tecnai G^2 F30 (FEI, USA) at 300kV with a point resolution of 0.20 nm. Both SEM and TEM were equipped with an EDX/EDS system. All FT-IR spectra were recorded using FT-IR spectrometer (Nicolet 170, SXFT/IR spectrometer, USA) from KBr discs in the range of 4000–400 cm^{-1}. Thermogravimetric analysis (TG) of CMC-Cu gel powder was determined by STA6000 (Perkin-Elmer, USA) under a helium flow of 50mL min^{-1} coupled with mass spectrometry analysis (SQ8MS, Perkin-Elmer) of evolved gases with m/z scanning range set as 16~500. The sample (12 mg) was heated from 40 °C to 600 °C at a heating rate of 10 °C min^{-1}. The MS ion source (70 eV) was maintained at 250 °C and temperature of injection port was set at 280 °C under a helium carrier. Differential scanning calorimetry (DSC) of CA@PC and Cu@PC were determined by CDR-4P (INESA Instrument, China) with 10 °C min^{-1} while heated up to 500°C in air atmosphere. The decomposition temperatures were given as peak maximum temperature. X-ray photoelectron spectroscopy (XPS) measurements were performed with a Thermo Scientific Escalab 250Xi using the monochromatic Al Ka line (1486.7 eV). Powder X-ray diffraction patterns were carried out with a Bruker D8 Advance diffractometer using Cu Ka radiation (λ = 1.5406 Å) at 40 kV and 40 mA. C, N and H contents were measured by EuroEA Elemental Analyser. Cu content was measured by PE optima 7000 with standard curve method.

ASSOCIATED CONTENT

Supporting Information.

The supporting information is available free of charge on ACS Publications website at.

Detail method and data on the calculations, additional characterization data, supporting table and

figures (Tables S1 and Figures S1−S16) (PDF)

Video showing brief description (AVI)

AUTHOR INFORMATION

Corresponding Author

* E-mail: yanglibit@bit.edu.cn.

Author contributions

[†1] These authors contributed equally.

Notes

The authors declare no competing financial interest.

ACKNOWLEDGMENT

We gratefully acknowledge financial support from the National Natural Science Foundation of China (No. 11672040), the State Key Laboratory of Explosion Science and Technology (No. YB2016-17), and Beijing Institute of Technology Research Fund Program for Young Scholars. The authors thank M.A. Qi Zhao (Central Academy of Fine Arts) for providing ideas of schematics. The authors also thank M.S. Jin Xu (School of Life Science, Beijing Institute of Technology) for ideas of self-healable experiment.

REFERENCES

(1) Fronabarger, J. W.; Williams, M. D.; Sanborn, W. B.; Bragg, J. G.; Parrish, D. A.; Bichay, M. DBX–1–A Lead Free Replacement for Lead Azide. Propell. Explos. Pyrot. **2011**, 36, 541-550.

(2) Barsan, M. E.; Miller, A. National Institute for Occupational Safety and Health. Lead Health Hazard Evaluation HETA Report No. 91-0346-2572. Cincinnati, Ohio. **1996**.

(3) Giles J. Green explosives: collateral damage. *Nature* **2004**, *427*, 580-581.

(4) Dan Chen, Hongwei Yang, Zhenxin Yi. C8N26H4: An Environmentally Friendly Primary Explosive with High Heat of Formation. Angew. Chem. Int. Ed. **2018**, 57, 2081-2084.

(5) Wei Li, Kangcai Wang, Qinghua Zhang. Construction of a Thermally Stable and Highly Energetic Metal–Organic Framework as Lead-Free Primary Explosives. Crystal Growth & Design. **2018**, 18, 1896-1902.

(6) Fischer, D.; Klapötke, T. M.; Stierstorfer, J. 1, 5□Di (nitramino) tetrazole: High Sensitivity and Superior Explosive Performance. *Angew. Chem. Int. Ed.* **2015**, *54*, 10299-10302.

(7) He, C.; Shreeve, J. M. Potassium 4, 5□Bis (dinitromethyl) furoxanate: A Green Primary Explosive with a Positive Oxygen Balance. *Angew. Chem. Int. Ed.* **2016**, *55*, 772-775.

(8) Tang, Y.; Gao, H.; Mitchell, L. A.; Parrish, D. A.; Shreeve, J. M. Enhancing Energetic Properties and Sensitivity by Incorporating Amino and Nitramino groups into a 1, 2, 4□Oxadiazole Building Block. *Angew. Chem. Int. Ed.* **2016***, 55,* 1147 –11502.

(9) Fedoroff, B. T.; Sheffield, O. E.; Clift, G. D.; Reese, E. F. *Encyclopedia of Explosives and Related Items (No. PA-TR-2700)*; Picatinny Arsenal: Dover, **1966**; Vol. 6, pp. 217–223.

(10) Fair, H. D.; Walker, R. F. *Energetic materials*; Plenum Publishing Corporation: New York, **1977**; Vol. 1; pp 53-57.

(11) Cartwright, M, Wilkinson, J. Correlation of Structure and Sensitivity in Inorganic Azides I Effect of Non-Bonded Nitrogen Nitrogen Distances. *Propell. Explos. Pyrot.* **2010**, *35*, 326-332.

(12) Zhu, W.; Xiao, H. Ab initio study of energetic solids: Cupric azide, mercuric azide, and lead azide. *J. Phys. Chem.* **2006**, *110*, 18196-18203.

(13) Li, Z. M.; Zhou, M. R.; Zhang, T. L.; Zhang. J. G.; Yang, L.; Zhou, Z. N. The facile synthesis of graphene nanoplatelet–lead styphnate composites and their depressed electrostatic hazards. *J. Mater. Chem.* **2013**, *1*, 12710-12714.

(14) Matyáš R.; Šelešovský J.; Musil T. Sensitivity to friction for primary explosives. *J. Hazard Mater.* **2012**, *213*, 236-241.

(15) Assovskiy, I G. Metallized SWCNT–Promising Way to Low Sensitive High Energetic Nanocomposites. *Propell. Explos. Pyrot.* **2008**, *33*, 51-54.

(16) Zhang, F.; Wang, Y.; Bai, Y.; Zhang, R. Preparation and characterization of copper azide nanowire array. *Mater. Lett.* **2012**, *89*, 176-179.

(17) Pelletier, V.; Bhattacharyya, S.; Knoke, I.; Forohar, F.; Bichay, M.; Gogotsi, Y. Copper azide confined inside templated carbon nanotubes. *Adv. Func. Mater.* **2010**, *20*, 3168-3174.

(18) Wang, Q.; Feng, X.; Wang, S.; Song, N.; Chen, Y.; Tong, W.; Yang, L; Wang, B. Metal□Organic Framework Templated Synthesis of Copper Azide as the Primary Explosive with Low Electrostatic Sensitivity and Excellent Initiation Ability. *Adv. Mater.* **2016**, *28*, 5837-5843.

(19) Raymundo□Piñero, E.; Leroux, F.; Béguin, F. A high-performance carbon for supercapacitors obtained by carbonization of a seaweed biopolymer. *Adv. Mater.* **2006**, *18*, 1877-1882.

(20) László, K.; Bóta, A.; Nagy, L. G. Comparative adsorption study on carbons from polymer precursors. *Carbon*, **2000**, *38*, 1965-1976.

(21) Paris, O.; Zollfrank, C.; Zickler, G. A. Decomposition and carbonisation of wood biopolymers—a microstructural study of softwood pyrolysis. *Carbon*, **2005**, *43*, 53-66.

(22) Liu, Q.; Lv, C.; Yang, Y.; He, F.; Ling, L. Study on the pyrolysis of wood-derived rayon fiber by thermogravimetry–mass spectrometry. *J. Mol. Struct.* **2005**, *733*, 193-202.

(23) Sun, J. Y.; Zhao, X.; Illeperuma, W. R.; Chaudhuri, O.; Oh, K. H.; Mooney, D. J.; Joost J. V.; Suo, Z. Highly stretchable and tough hydrogels. *Nature*, 2**012**, *489*, 133-136.

(24) Meng, H.; Xiao, P.; Gu, J.; Wen, X.; Xu, J.; Zhao, C.; Zhang, J.; Chen, T. Self-healable macro-/microscopic shape memory hydrogels based on supramolecular interactions. *Chem. Commun.* **2014**, *50*, 12277-12280.

(25) Wei, Z.; Yang, J. H.; Liu, Z. Q.; Xu, F.; Zhou, J. X.; Zrínyi, M.; Osada Y.; Chen, Y. M. Novel Biocompatible Polysaccharide□Based Self□Healing Hydrogel. *Adv. Func. Mater.* **2015**, *25*, 1352-1359.

(26) Li, N.; Bai, R. Copper adsorption on chitosan–cellulose hydrogel beads: behaviors and mechanisms. Separation and purification technology, *Sep. Purif. Technol*. **2005**, *42*, 237-247.

(27) Suh, J. K. F.; Matthew, H. W. Application of chitosan-based polysaccharide biomaterials in cartilage tissue engineering: a review. *Biomaterials* **2000**, *21*, 2589-2598.

(28) Ishihara, M.; Nakanishi, K.; Ono, K.; Sato, M.; Kikuchi, M.; Saito, Y.; ; Kurita, A. Photocrosslinkable chitosan as a dressing for wound occlusion and accelerator in healing process. *Biomaterials* **2002**, *23*, 833-840.

(29) Song, Y.; Zhou, J.; Zhang, L.; Wu, X. Homogenous modification of cellulose with acrylamide in NaOH/urea aqueous solutions. *Carbohydrate polymers* **2008**, *73*, 18-25.

(30) Liu, Y.; Wang, W.; Wang, A. Adsorption of lead ions from aqueous solution by using carboxymethyl cellulose-g-poly (acrylic acid)/attapulgite hydrogel composites. *Desalination*, **2010**, *259*, 258-264.

(31) Wang, W.; Wang, A. Nanocomposite of carboxymethyl cellulose and attapulgite as a novel pH-sensitive superabsorbent: Synthesis, characterization and properties. *Carbohydr. Polym.* **2010**, 82, 83-91.

(32) Peppas, N. A.; Hilt, J. Z.; Khademhosseini, A.; Langer, R. Hydrogels in biology and medicine: from molecular principles to bionanotechnology. *Adv.Mater.* **2006**, *18*, 1345-1360.

(33) Yuan, X.; Marcano, D. C.; Shin, C. S.; Hua, X.; Isenhart, L. C.; Pflugfelder, S. C.; Acharya, G. Ocular drug delivery nanowafer with enhanced therapeutic efficacy. *ACS nano* **2015**, *9*, 1749-1758.

(34) Grasdalen, H.; Larsen, B.; Smisrod, O. 13 CN. MR studies of monomeric composition and sequence in alginate. *Carbohydr. Res.* **1981**, *89*, 179-191.

(35) Zhong, M.; Liu, X. Y.; Shi, F. K.; Zhang, L. Q.; Wang, X. P.; Cheetham, A. G.; Cuib, H.; Xie, X. M. Self-healable, tough and highly stretchable ionic nanocomposite physical hydrogels. *Soft matter* **2015**, *11*, 4235-4241.

(36) Kuo, C. K.; Ma, P. X. Ionically crosslinked alginate hydrogels as scaffolds for tissue engineering: Part 1. Structure, gelation rate and mechanical properties. *Biomaterials* **2001**, *22*, 511-521.

(37) Xia, W.; Zhu, J.; Guo, W.; An, L.; Xia, D.; Zou, R. Well-defined carbon polyhedrons prepared from nano metal–organic frameworks for oxygen reduction. *J. Mater. Chem. A* **2014**, *2*, 11606-11613.

(38) Li, S. L.; Xu, Q. Metal–organic frameworks as platforms for clean energy. *Energy Environ. Sci.* **2013**, *6*, 1656-1683.

(39) Xia, W., Qiu, B., Xia, D., & Zou, R. Facile preparation of hierarchically porous carbons from metal-organic gels and their application in energy storage. *Sci. Rep.* **2013**, *3*, 1935-1935.

(40) Hu, M.; Reboul, J.; Furukawa, S.; Torad, N. L.; Ji, Q.; Srinivasu, P.; Ariga, K.; Kitagawa, S.; Yamauchi, Y. Direct carbonization of Al-based porous coordination polymer for synthesis of nanoporous carbon. *J. Am. Chem. Soc.* **2012**, *134*, 2864-2867.

(41) Mathey, Y.; Greig, D. R.; Shriver, D. F. Variable-temperature Raman and infrared spectra of the copper acetate dimer $Cu_2(O_2CCH_3)_4(H_2O)_2$ and its derivatives. *Inorg. Chem.* **1982**, *21*, 3409-3413.

(42) Haldorai, Y.; Shim, J. J. Chemo-responsive bilayer actuator film: fabrication, characterization and actuator response. *New Journal of Chemistry*, **2014**, *38*, 2653-2659.

(43) Wu, F.; Zhang, Y.; Liu, L.; Yao, J. Synthesis and characterization of a novel cellulose-g-poly (acrylic acid-co-acrylamide) superabsorbent composite based on flax yarn waste. *Carbohydr. Polym.* **2012**, *87*, 2519-2525.

(44) Bellini, J. V.; Machado, R.; Morelli, M. R.; Kiminami, R. H. G. A. Thermal, structural and morphological characterisation of freeze-dried copper (II) acetate monohydrate and its solid decomposition products. *Materials Research* **2002**, *5*, 453-457.

(45) Bansode, R. R.; Losso, J. N.; Marshall, W. E.; Rao, R. M.; Portier, R. J. Adsorption of metal ions by pecan shell-based granular activated carbons. *Bioresource Technol.* **2003**, *89*, 115-119.

(46) Müller, T. G.; Karau, F.; Schnick, W.; Kraus, F. A New Route to Metal Azides. *Angew. Chem. Int. Ed.* **2014**, *53*, 13695-13697.

(47) Turrentine, J. W.; Moore, R. L. The Action of Hydronitric Acid on Cuprous Chloride and Metallic Copper. *J. Am. Chem. Soc.* **1912**, *34*, 382-384.

(48) Curtius, T. Ueber stickstoffwasserstoffsäure (azoimid) N_3H. *Ber. Dtsch. Chem. Ges.* **1890**, *23*, 3023-3033.

(49) Choi, J.; Gillan, E. G. Solvothermal synthesis of nanocrystalline copper nitride from an energetically unstable copper azide precursor. *Inorg. Chem.* **2005**, *44*, 7385-7393.

(50) Choi, W.; Hong, S.; Abrahamson, J. T.; Han, J. H.; Song, C.; Nair, N.; Baik, S.; Strano, M. S. Chemically driven carbon-nanotube-guided thermopower waves. *Nat Mater.* **2010**, *9*, 423-429.

(51) Zhang, G.; Sun, H.; Abbott, J. M.; Weeks, B. L. Engineering the microstructure of organic energetic materials. *ACS Appl.Mater.Interface* **2009**, *1*, 1086-1089.

(52) Mikulec, F. V.; Kirtland, J. D.; Sailor, M. J. Explosive nanocrystalline porous silicon and its use in atomic emission spectroscopy. *Adv. Mater.* **2002**, *14*, 38-41.

(53) Zou, J.; Li, X.; Lei, Y. Technology of in situ charge promotes the development of MEMS safety and arming device. *2nd IEEE International Conf. on Manipulation, Manufacturing and Measurement on the Nanoscale (IEEE-3M-NANO)*, **2012**, 244-249.

SYNOPSIS

An efficient primary explosive composed of porous carbon frameworks uniformly decorated with copper azide nanoparticles is fabricated based on ionic crosslinked hydrogel through a novel, green and facile strategy. The as-prepared hybrid exhibits much low electrostatic sensitivity and superior ignition ability, indicating the promising application in future functional energy-related fields.

For Table of Contents